EBioMedicine 46 (2019) 94–104

Contents lists available at ScienceDirect

EBioMedicine

journal homepage: www.ebiomedicine.com

EBioMedicine
Published by THE LANCET

The cellular prion protein controls the mesenchymal-like molecular subtype and predicts disease outcome in colorectal cancer

Delphine Le Corre [a,1], Alexandre Ghazi [a,1], Ralyath Balogoun [a], Camilla Pilati [a], Thomas Aparicio [b], Séverine Martin-Lannerée [a,2], Laetitia Marisa [c], Fatima Djouadi [a], Virginie Poindessous [a], Carole Crozet [d], Jean-François Emile [e], Claire Mulot [a], Karine Le Malicot [f], Valérie Boige [a,g], Hélène Blons [a,h], Aurélien de Reynies [c], Julien Taieb [a,i], François Ghiringhelli [j], Jaafar Bennouna [k], Jean-Marie Launay [l,m], Pierre Laurent-Puig [a,h], Sophie Mouillet-Richard [a,*]

[a] Centre de Recherche des Cordeliers, INSERM, Sorbonne Université, USPC, Université Paris Descartes, Université Paris Diderot, F-75006 Paris, France
[b] Department of Gastroenterology and Digestive Oncology, AP-HP, Hôpital Saint-Louis, Université Paris Diderot, F-75010 Paris, France
[c] Programme "Cartes d'Identité des Tumeurs", Ligue Nationale Contre le Cancer, F-75013 Paris, France
[d] Institut de Médecine Régénératrice et de Biothérapie (I.M.R.B.), Université de Montpellier UMR-1183, Centre Hospitalo-Universitaire de Montpellier, F-34000 Montpellier, France
[e] Department of Pathology, AP-HP, Hôpital Ambroise Paré, F-92100 Boulogne-Billancourt, France
[f] Fédération Francophone de Cancérologie Digestive, EPICAD INSERM LNC-UMR 1231, Université de Bourgogne et and Franche Comté, F-21000 Dijon, France
[g] Department of Cancer Medicine, Institut Gustave Roussy, Université Paris-Saclay, F-94800 Villejuif, France
[h] Department of Biology, AP-HP, Hôpital Européen Georges Pompidou, F-75015 Paris, France
[i] Department of Gastroenterology and GI Oncology, AP-HP, Hôpital Européen Georges Pompidou, F-75015 Paris, France
[j] Department of Medical Oncology, Centre Georges-François Leclerc, F-21000 Dijon, France
[k] Department of Medical Oncology, Institut de Cancérologie de l'Ouest, F-44800 Saint-Herblain, France
[l] Department of Biochemistry and Molecular Biology, INSERM U942, AP-HP, Hôpital Lariboisière, Université Paris Descartes, F-75010 Paris, France
[m] Pharma Research Department, F. Hoffmann-La-Roche Ltd., CH-4070 Basel, Switzerland

ARTICLE INFO

Article history:
Received 27 May 2019
Received in revised form 10 July 2019
Accepted 14 July 2019
Available online 31 July 2019

Keywords:
Colorectal cancer
Molecular classification
Prion protein
Hippo pathway
TGFß pathway

ABSTRACT

Background: Comprehensive transcriptomic analyses have shown that colorectal cancer (CRC) is heterogeneous and have led to the definition of molecular subtypes among which the stem-cell, mesenchymal-like group is associated with poor prognosis. The molecular pathways orchestrating the emergence of this subtype are incompletely understood. In line with the contribution of the cellular prion protein PrP^C to stemness, we hypothesize that deregulation of this protein could lead to a stem-cell, mesenchymal-like phenotype in CRC.

Methods: We assessed the distribution of the PrP^C-encoding *PRNP* mRNA in two large CRC cohorts according to molecular classification and its association with patient survival. We developed cell-based assays to explore the impact of gain and loss of PrP^C function on markers of the mesenchymal subtype and to delineate the signalling pathways recruited by PrP^C. We measured soluble PrP^C in the plasmas of 325 patients with metastatic CRC and probed associations with disease outcome.

Findings: We found that *PRNP* gene expression is enriched in tumours of the mesenchymal subtype and is associated with poor survival. Our in vitro analyses revealed that PrP^C controls the expression of genes that specify the mesenchymal subtype through the recruitment of the Hippo pathway effectors YAP and TAZ and the TGFß pathway. We showed that plasma levels of PrP^C are elevated in metastatic CRC and are associated with poor disease control.

Interpretation: Our findings define PrP^C as a candidate driver of the poor-prognosis mesenchymal subtype of CRC. They suggest that PrP^C may serve as a potential biomarker for patient stratification in CRC.

Funding: Grant support was provided by the following: Cancéropôle Ile de France (grant number 2016-1-EMERG-36-UP 5-1), Association pour la Recherche sur le Cancer (grant number PJA 20171206220), SATT Ile de France Innov (grant number 415) as well as INSERM.

* Corresponding author at: INSERM UMR-S 1138, Centre de Recherche des Cordeliers, INSERM, Sorbonne Université, USPC, Université Paris Descartes, Université Paris Diderot, 15 rue de l'Ecole de Médecine, F-75006 Paris, France.
E-mail address: sophie.mouillet-richard@parisdescartes.fr (S. Mouillet-Richard).
[1] These authors contributed equally.
[2] Present address: IntegraGen SA Génopole Campus 1, Rue de Henri Desbruères 91000 Evry France.

https://doi.org/10.1016/j.ebiom.2019.07.036

Research in context

Evidence before the study

Colorectal cancer is a heterogeneous disease that can be classified into distinct molecular subtypes. Among those, the stem cell-like, mesenchymal-like subtype is associated with poor prognosis. The molecular pathways sustaining this phenotype are incompletely understood. The cellular prion protein PrP^C is over-expressed in several cancers and is emerging as a potential marker of cancer stem cells.

Added value of this study

Using two large cohorts of colorectal cancer, we document that expression of the *PRNP* gene encoding PrP^C is elevated in tumours of the mesenchymal subtype and that high *PRNP* levels are associated with poor survival. Through gain and loss of function approaches in colorectal cancer cell lines, we show that PrP^C controls the expression of a panel of genes that specify the mesenchymal subtype and that this action is relayed by the Hippo effectors YAP/TAZ and by the TGFß pathway. We measured high levels of circulating PrP^C in the plasma of patients with metastatic colorectal cancer as compared with healthy subjects and we found that high plasma levels of PrP^C are correlated with poor disease control.

Implication of all the available evidence

These findings suggest that PrP^C could be a relevant biomarker for the prognostication of patients with colorectal cancer as well as a potential therapeutic target.

1. Introduction

Colorectal cancer (CRC) is one of the five most frequent cancers and a leading cause of cancer-associated death worldwide. Over the past years, pioneering studies based on high-throughput profiling technologies have allowed to uncover CRC heterogeneity and to classify tumours into several subgroups according to gene expression patterns [1–6]. Among these, our group has contributed to define 6 molecular subtypes based on transcriptome analysis of a large cohort of patients with stage I to IV colon cancer [3]. We further took part to the international CRC Subtyping Consortium that established a consensus classification [7]. Although these overall studies have allowed much progress in our understanding of the diversity of CRC, our knowledge of the signalling pathways that selectively drive each molecular subtype is still incomplete. This notion most notably applies to the C4 subgroup in the Marisa classification, and to the larger CMS4 subgroup into which it is included in the consensus classification. Because one hallmark of the C4/CMS4 tumours is a cancer stem cell (CSC) like and/or an Epithelial-Mesenchymal Transition (EMT) signature, we may expect that some CSC markers contribute to control their phenotype. One emerging regulator of CSC function is the cellular prion protein PrP^C [8], which is infamous for its involvement in a group of neurodegenerative diseases under its pathogenic scrapie isoform [9]. PrP^C is a ubiquitous protein mainly found as a GPI-anchored cell surface molecule and also present in the extracellular space as a soluble isoform [10]. PrP^C can interact with promiscuous partners and mobilize cell signalling cascades [10], which make it an interesting candidate to sense the tumour microenvironment and foster an adaptive response in cancer cells.

By exploiting two large cohorts of CRC patients, we substantiate a significant up-regulation of the PrP^C-encoding gene *PRNP* in tumours exhibiting a C4/CMS4 signature and that high *PRNP* expression is associated with a poor prognosis. By combining in silico analyses and cell-based assays, we provide evidence that PrP^C controls the expression of a panel of genes that specify the C4/CMS4 phenotype and that PrP^C operates through an activation of the YAP/TAZ and the TGFß pathways. Finally, we found that plasma levels of PrP^C predict disease control in metastatic CRC.

2. Materials and methods

2.1. Reagents

All tissue culture reagents were from Invitrogen (Carlsbad, CA, USA). SB431542, Verteporfin, 5-Fluorouracil and mouse monoclonal antibody against α-tubulin were from Sigma-Aldrich (St. Louis, MO, USA). Polyclonal rabbit antibodies against phospho-YAP (S127) were from Cell Signalling Technology (Danvers, MA, USA). Mouse monoclonal antibodies against PrP^C (Sha31) were from SPI-Bio (Montigny Le Bretonneux, France). Mouse monoclonal antibodies against YAP were from Santa Cruz (Santa Cruz, CA, USA). Recombinant TGFß1 was from R&D systems (Minneapolis, MN, USA). ELISA for soluble TGFß1 was from Biolegend (San Diego, CA, USA).

2.2. Cell culture

The human CRC MDST8 and LoVo cell lines were purchased from Sigma. MDST8 cells were grown in DMEM with 10% fetal bovine serum. LoVo cells were grown in F-12 K medium supplemented with 10% fetal bovine serum. All cell lines were grown at 37 °C and 5% CO_2 in a humidified incubator and regularly tested for mycoplasma contamination. For transient siRNA-mediated silencing, cells were transfected with siRNA sequences (30 nM) using the Lipofectamine 2000 reagent according to the manufacturer's instructions (Invitrogen). Specific siRNA sequences used were: 5′-CAGUACAGCAACCAGAACATT-3′ (sense siPRNP) 5′-AACGAUGACACGAACACACTT-3′ (sense scramble), 5′-GCCACCAAGCUAGAUAAAGAATT-3′ (sense siYAP), 5′-CAGCCAAAU CUCGUGAUGAAUTT-3′ (sense siTAZ) and 5′-AGAUAACGCACACCAA GUAAGTT-3′ (sense scramble). Cellular mRNAs or protein extracts were collected 72 h after PrP^C silencing or 48 h after YAP and/or TAZ silencing. For PrP overexpression, LoVo cells were transfected with 2.5 μg of the pcDNA3-prnp plasmid that expresses mouse *Prnp* (kind gift of Pr. Sylvain Lehmann) using the Lipofectamine 3000 reagent according to the manufacturer's instructions (Invitrogen). The corresponding empty vector was used as control. Mouse *Prnp* was chosen instead of human *PRNP* for biosafety considerations. Due to high conservation, PrP^C from different species can functionally substitute for each other [11].

2.3. Preparation of protein extracts and western blot analyses

Cells were washed in PBS and incubated for 30 min at 4 °C in NaDOC lysis buffer [50 mM Tris·HCl (pH 7.4)/150 mM NaCl/5 mM EDTA/0.5% Triton X-100/0.5% sodium deoxycholate] and a mixture of phosphatase (Thermo-Scientific, Waltham, MA, USA) and protease (Roche, Mannheim, Germany) inhibitors. Extracts were centrifuged at 14,000 xg for 15 min. Protein concentrations in the supernatant were measured by using the bicinchoninic acid method (Pierce, Rockford, IL, USA). Protein extracts (15 μg) were resolved by 4–12% SDS-PAGE (Invitrogen) and transferred to nitrocellulose membranes (iBlot, Invitrogen). Membranes were blocked with SEABLOCK blocking buffer (Thermo-Scientific) for 1 h at room temperature and then incubated overnight at 4 °C with primary antibody. Bound antibody was revealed by infrared detection using a secondary antibody coupled to IRDye fluorophores (Li-Cor

biosciences, Lincoln, NE, USA). Western blot read out was performed with the Odyssey Infrared Imaging System (Li-Cor biosciences).

2.4. Isolation of total RNA and RT-PCR analysis

RNA was isolated by using the RNeasy extraction kit (Qiagen, Limburg, Netherlands), as recommended by the manufacturer's instructions. For reverse transcriptase-polymerase chain reaction (RT-PCR) analysis, first-strand cDNA was synthesized with oligo(dT) primer and random 6mers, using the High-capacity cDNA Reverse Transcription (Applied Biosystems) according to the manufacturer's protocol. Real-time PCR was performed using Absolute QPCR SYBR Green ROX Mix (Thermo-Scientific, Waltham, MA, USA) on a ABI PRISM 7900HT (Applied Biosystems, Life Technologies Corporation, Carlsbad, CA, USA). Real-time PCR analyzes was performed with the SDS software 2.3 (Applied biosystems). Primers used for the PCR reactions are shown on Table S1. Results are expressed as a relative quantification of a target gene transcript normalized to the *RPL13A* housekeeping gene using the ΔΔCt method.

2.5. Cell proliferation and viability assays

Cells were seeded in 96-well plates and transfected with siRNA against *PRNP* 24 h post seeding. After another 24 h, culture medium was replaced by fresh medium containing siRNA and 5-FU dissolved in DMSO at the indicated concentrations. After 48 h of incubation, 20 μL of MTS (Lonza, Allendale, NJ, USA) was added in 100 μL of culture medium and incubated for 1 h in 37 °C 5% incubators protected from light. Fluorescence intensity was measured with a plate reader (infinite®-M200, Tecan). Background fluorescence was subtracted from each data point and cell viability at each concentration was expressed as a fraction of untreated (DMSO) control wells. IC_{50} was defined as the concentration where 50% of the maximum effect was reached.

For cell counting experiments, cells (2×10^5) were seeded in 6-well plates and transfected with siRNA against *PRNP* 24 h post seeding. After another 24 h, culture medium was replaced by fresh medium containing siRNA and 5-FU dissolved in DMSO at 200 μM. After 48 h of incubation, cells from three wells per group were harvested and total cell numbers (cells/well) were determined using a CASY.TT cell counter (Schärfe System GmbH, Reutlingen, Germany). Cells transfected with control siRNA and treated with vehicle (DMSO) were used as reference for normalization.

2.6. Gene expression analyses

All data analysed were retrieved from the following public sources: GSE39582 ("CIT cohort"), GSE13294, GSE18088, GSE14333, GSE13067, GSE17536, GSE17537, GSE33113, GSE26682, GSE5851, TCGA, altogether forming the "validation cohort". Subtype classification systems assignments were performed using original published predictor methods as described in [3,7].

To generate Kaplan-Meier plots, samples were grouped according to *PRNP* gene expression with a threshold corresponding to the 90th percentile of non-tumours samples. Kaplan-Meier plots were then generated for the respective groups using the "survival" (Cancer Genome Atlas Network, 2012) R package.

2.7. Gene set enrichment analysis (GSEA)

GSEA [12] was performed on the following data sets: TCGA colon [13] and GSE39582 [3] for patients and GSE59857 [14] for cell lines. The GSEA was performed using the Broad Institute platform (http://www.broadinstitute.org/gsea/index.jsp; Version 2.0.14), using the *PRNP* gene as a phenotype.

2.8. Collection of blood samples and analysis of plasma PrP^C

Plasma samples were collected within the PRODIGE9 trial, a randomized phase III trial comparing the impact of Bevacizumab maintenance versus no treatment during chemotherapy-free intervals in metastatic colorectal cancer [15]. As no difference was observed in experimental and control arm for disease control duration, progression free survival and overall survival, we assume to pool the patients from both arms in the present analysis. Among the 488 patients assigned within the trial, blood samples were obtained for 325 patients before the start of treatment (see baseline patient characteristics in Table S2). Collection of material was approved by the Ethics Committee for the Protection of Persons Ile de France VIII. The patients, for which informed written consent had been obtained, and methods for the PRODIGE9 trial have been described previously (trial registration number NCT00952029) [16]. Blood samples of 32 age-matched healthy individuals without any indication of malignancy were collected as a control group. All plasma samples were frozen at −70 °C until analysis. The levels of PrP^C were quantified in plasmas by DELFIA as in [17]. Experiments were all carried out under blinded conditions.

2.9. Statistical analysis

The results are reported as the means ± standard errors of the means (s.e.m.). The unpaired Student's *t*-test or the ANOVA variance analysis with Tukey post hoc test were used for group comparisons. Survival curves were obtained using Kaplan-Meier estimates and differences between groups of patients were assessed using the log-rank test for univariate analyses or Cox models for multivariate analyses. A p-value <.05 was considered significant.

3. Results

3.1. PrP^C expression is enriched in mesenchymal colorectal tumours and is associated with poor prognosis

In order to assess expression of the PrP^C-encoding gene *PRNP* according to colon cancer diversity, we exploited transcriptome analysis data of a large cohort of patients ($n = 566$) with stage I to IV CRC (CIT cohort), which allowed us to define a molecular classification into 6 subtypes (C1 to C6) [3]. Our dataset was further included in the international CRC Subtyping Consortium study that produced a consensus classification (CMS1 to CMS4) [7]. As a validation cohort, we combined several public CRC datasets, altogether reaching $n = 1682$ patients, among which $n = 1029$ and $n = 1022$ could be ascribed a "Marisa" and a consensus classification subtype, respectively. When examining the distribution of *PRNP* expression levels according to the two classification subtypes, *PRNP* mRNA levels were significantly elevated in the C4 ("Marisa" classification) (Fig. 1a and b) and CMS4 (consensus classification) (Fig. 1c and d) subgroups, respectively. Beyond our own study and that of the CRC subtyping consortium, several other groups have proposed diverse CRC classifications, which differ according to the number of subtypes and gene classifiers [1–6]. Whatever the classification system used, *PRNP* levels were significantly higher in the worse-prognosis subgroup (Fig. S1). In line with this, samples with high *PRNP* levels were associated with a worse outcome in terms of overall survival (Fig. 1e) and relapse-free survival (Fig. 1f) in the CIT cohort. Thus, we may conclude that *PRNP* expression is elevated in the C4/CMS4 subgroup of CRC and is associated with poor prognosis.

3.2. PrP^C contributes to the mesenchymal stem-like signature of colorectal cancer

Since PrP^C is found at the cell surface molecule and can instruct cell signalling events [10], we wondered whether it would control the expression of genes that specify the C4/CMS4 phenotype of CRC. First,

when examining the genes most correlated with *PRNP* expression in in 3 different CRC studies, namely The Cancer Genome Atlas (TCGA) [13] and the study by Marisa [3] for patients and the study by Medico [14] carried out on a panel of CRC cell lines, we found significant correlation indexes between the levels of *PRNP* and those of 8 out of 10 genes that define the C4 centroid (Fig. 2a), supporting the link between PrP^C and the C4 subtype. Next, we selected a set of genes for their high correlation with *PRNP* levels in the Marisa [3] and/or the Medico [14] studies and for their selective up-regulation in the C4 subgroup [18] (Fig. 2b). Regarding the CMS classification, we based our selection on the recently introduced "CMScaller" classifier that provides a list of genes that specify each subtype [19], some of which overlap with the C4-enriched PrP^C-associated genes (Fig. 2c). All these genes exhibited high correlation indexes with *PRNP* expression in CRC studies (Fig. 2d). Interestingly, in TCGA samples, COL6A1, which belongs to the CMS4 classifier, represents the 3rd protein whose level is most correlated with *PRNP* mRNA levels (Pearson's correlation coefficient $R = 0.33$, $p < .00001$).

To evaluate whether PrP^C would control the expression of C4/CMS4 genes, we assessed the impact of PrP^C silencing in the MDST8 colon cancer cell line, which expresses high level of PrP^C both at the mRNA [14] and protein level [20] and displays a C4/CMS4 phenotype (Table S3 and [19]). We found that PrP^C depletion in MDST8 cells promoted significant reductions in the levels of the selected transcripts (Fig. 2e). In a complementary approach, we examined the impact of PrP^C overexpression in a non-C4/CMS4 cell line. We selected LoVo cells, which belong to the C2 (Table S3) and CMS1 subgroups [19], and exhibit <15% of the PrP^C level found in MDST8 cells according to the CRC proteomics panel [20]. We found that, in a time-window ranging from 3 to 5 days post-transfection, the levels of the C4/CMS4 genes tested were significantly increased in PrP^C-overexpressing LoVo cells, except for *ITGA5*, *DDR2* and *ITGB5*, which were significantly decreased (Fig. 2f).

Finally, because one hallmark of CMS4 cell lines is their increased resistance to 5-FU [19], we probed a link between PrP^C expression and resistance to 5-FU. When examining the relative sensitivity of a panel of CRC cell lines [21] as a function of *PRNP* gene expression [14] or PrP^C protein expression [20], we found that the group of 5-FU resistant cell lines was associated with significantly higher expression of PrP^C, both at the mRNA and protein levels (Fig. S2a and b). Cell viability assays further revealed that siRNA-mediated PrP^C depletion in MDST8 cells reduced the IC_{50} for 5-FU (48 h) from 340 μM to 265 μM (Fig. S2c). Accordingly, cell counting indicated that the decrease in cell number (65%) and cell viability (19%) monitored in MDST8 cells exposed to 5-FU was amplified upon siRNA-mediated depletion of PrP^C (78% and 28% reductions for cell number and viability, respectively) (Fig. S2d). Overall, these data indicate that PrP^C controls molecular features specific to the C4/CMS4 subtype in colon cancer cell lines.

3.3. The PrP^C-YAP/TAZ axis contributes to the mesenchymal stem-like signature of colon cancer

In a next step, we sought to delineate the molecular cascade through which PrP^C controls the expression of C4/CMS4 genes. We conducted gene set enrichment analyses (GSEA) in order to determine the pathways enriched among the genes most correlated with *PRNP* gene expression. We found that the expression of *PRNP* was highly associated with the "YAP conserved signature" and the "YAP-up" signature in the TCGA colon, Marisa and Medico studies (Fig. 3a and b). This indicates that the genes most correlated with *PRNP* gene expression are enriched in genes associated with the activation of YAP/TAZ. YAP and its paralogue TAZ are two effectors of the Hippo pathway that shuttle between the cytoplasm and the nucleus where they bind transcription factors and modulate their activity [22]. Phosphorylation of YAP/TAZ is associated with their cytoplasmic retention and/or degradation whereas their nuclear translocation allows the activation of a YAP/TAZ-dependent transcriptional program [22]. Interestingly, YAP and TAZ proteins are selectively elevated in the CMS4 subgroup [7]. In further support for a link between PrP^C and YAP/TAZ, we observed that, in TCGA samples, YAP and TAZ feature among the top-10 proteins whose levels are significantly correlated with *PRNP* mRNA levels (Fig. 3c). In addition, the *PRNP* expression levels in CRC studies correlated with those of *YAP1* and *WWTR1*, encoding TAZ, as well as their target genes *CYR61*, *CTGF* and *AXL* (Fig. 3d and e). Finally, we found that most of the C4/CMS4 genes under the control of PrP^C are either YAP/TAZ occupied genes [23,24] or positively regulated by YAP [25] (Fig. S3a).

In MDST8 cells, PrP^C depletion promoted a significant reduction (31%) in the levels of TAZ, and an increase in the ratio phosphorylated YAP to total YAP, suggesting reduced activity of YAP/TAZ in the absence of PrP^C (Fig. 3f). We further observed decreased expression of a set of YAP/TAZ target genes in PrP^C–silenced MDST8 cells (Fig. 3g). We confirmed that these genes are indeed YAP/TAZ targets in this particular cell context since their levels are all importantly reduced upon inhibition of the YAP/TAZ-TEAD transcription complex by Verteporfin or upon YAP and/or TAZ silencing (Fig. S3b and c). Finally, we found that YAP or TAZ silencing promoted a significant down-regulation of most of the PrP^C-regulated, C4/CMS4-associated genes (Fig. 3h). These data thus delineate a PrP^C-YAP/TAZ axis in CRC and point to YAP/TAZ as a relay of the PrP^C-dependent control on C4/CMS4 genes.

3.4. TGFß signalling contributes to the PrP^C-dependent action in C4/CMS4 colon cancer cells

We next sought to probe a potential link between PrP^C and EMT and the TGFß axis since they are two major pathways that distinguish the C4 and CMS4 subgroups in CRC [3,7], including in pre-clinical models, i.e. in the absence of stroma [19]. We first observed that EMT and the TGFß signalling pathway feature among those that are associated with *PRNP* gene expression in the TCGA, Marisa and Medico studies (Fig. 4a and b). PrP^C silencing in MDST8 cells further promoted a reduction in the levels of *TGFB1* mRNAs as well as soluble TGFß1 (Fig. 4c). To the opposite, we monitored progressive increases in the level of soluble TGFß1 in *Prnp*-overexpressing LoVo cells, reaching 277% of control 5 days post-transfection (Fig. 4d). In order to assess the relative contribution of TGFß signalling on the PrP^C-dependent action in C4/CMS4 colon cancer cells, we examined the impact of biochemical blockade of the pathway using the TGF-βRI antagonist SB431542. We first monitored a reduction in *TGFB1* transcripts in MDST8 cells exposed to SB431542 (Fig. S4a), in line with *TGFB1* being a target of its own pathway [18] and thereby confirming the efficacy of TGFß pathway blockade. In addition, SB431542 promoted a mild but significant decrease in *PRNP* mRNAs (Fig. S4a). This observation recalls the induction of *PRNP* in response to TGFß in endothelial cells reported by Calon et al. [18]. Next, we reasoned that if the reduction of soluble TGFß1 in the supernatant of PrP^C-silenced cells contributes to the decrease in the levels of C4/CMS4 genes, then those alterations should be rescued after TGFß1 addition. We thus assessed the outcome of exogenous addition of TGFß1 in MDST8 cells, with or without prior silencing of PrP^C. In accordance with the data obtained with SB431542, MDST8 cells exposed to TGFß1 exhibited increased levels of *TGFB1* and *PRNP* mRNAs (Fig. S4b). As for the PrP^C-C4/CMS4 axis, we observed decreases in *FRMD6*, *PDGFC*, *ITAG5*, *ITGB5*, *AXL*, *CDH2*, *COL6A1*, *ZEB1* and *CTGF* after TGF-βRI inhibition (Fig. 4e). Consistently, the impact of TGFß1 addition on genes of the PrP^C-C4/CMS4 axis was also globally the opposite of that of SB431542 (Fig. 4f). Notably, exogenous TGFß1 rescued the expression of *FRMD6*, *PDGFC*, *ITGA5*, *ITGB5*, *AXL*, *CDH2*, *COL6A1*, *ZEB1* and *CTGF* in *PRNP*-silenced MDST8 cells. As a whole, our data argue that TGFß1 represents one of the effectors of PrP^C that contribute to its action in the control of C4/CMS4 genes.

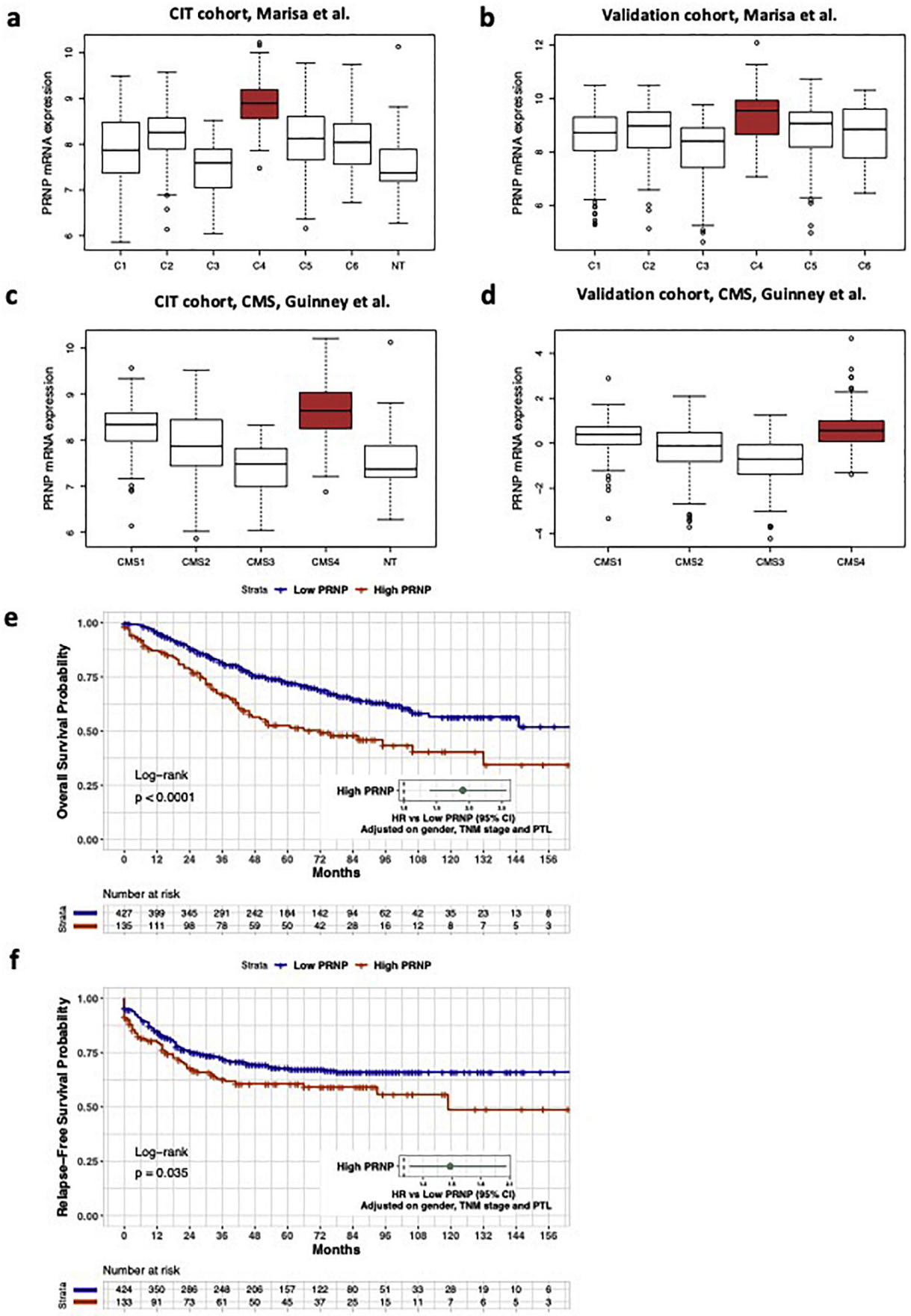

Fig. 1. *PRNP* expression is elevated in C4/CMS4 CRC and is associated with poor prognosis. (a-d) Relative *PRNP* gene expression in patients from the CIT cohort (a,c) or the validation cohort (b,d) within the 6 molecular subgroups of the "Marisa classification" (a,b) or the 4 molecular subgroups of the consensus classification (c,d). NT: non-tumours controls. $p < .0001$ for C4 or CMS4 versus all other subtypes in (a,c). $p < .01$ for CMS4 versus CMS1, $p < .005$ for C4 versus C2, C5 and C6 and $p < .0001$ for C4 or CMS4 versus all other subtypes in (b,d). (e-f) Kaplan-Meier overall survival (e) and relapse free survival (f) according to high and low *PRNP* gene expression was determined in the CIT cohort.

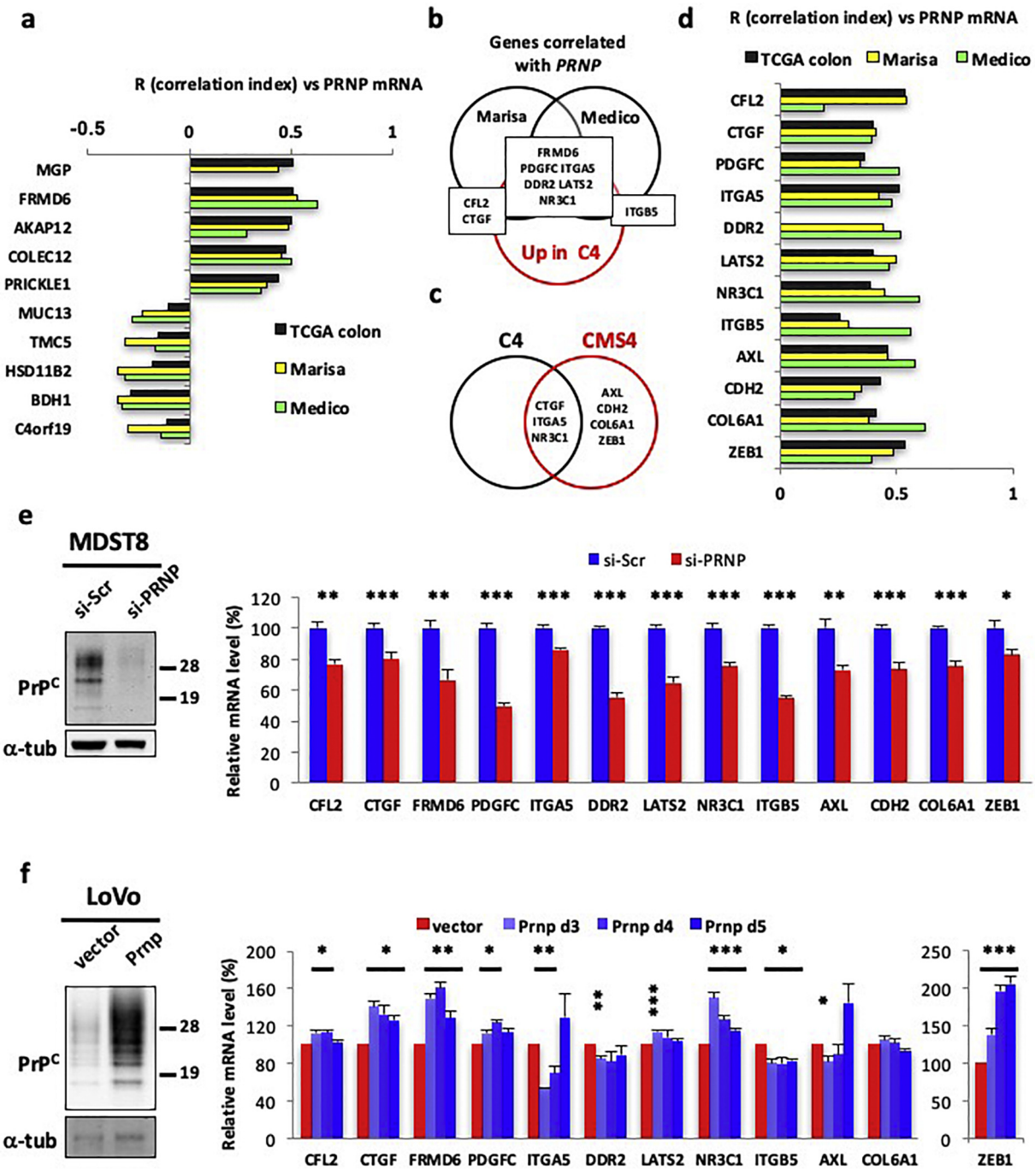

Fig. 2. PrP^C contributes to the C4/CMS4 signature of CRC. (a) Correlations indexes (R, Pearson) between mRNA expression of *PRNP* and that of genes of the C4 centroid in the TCGA colon, Marisa and Medico studies. *PRNP* levels are positively correlated to those of 4 of the genes positively defining the C4 centroid (*FRMD6*, *AKAP12*, *COLEC12* and *PRICKLE1*) and are negatively correlated to those of 4 of genes negatively defining the C4 centroid (*MUC13*, *TMC5*, *HSD11B2* and *BDH1*). *FRMD6* was selected for further analysis since it has the highest correlation levels with *PRNP* expression. (b) A set of genes was selected on the basis of the following criteria: high level of correlation with *PRNP* expression in the Marisa [3] and/or the Medico [14] studies (R Pearson >0.40) and enrichment in the C4 subgroup [18]. (c) A set of genes was selected according to their enrichment in the CMS4 subgroup as in [19]. (d) Correlations indexes (R, Pearson) between mRNA expression of *PRNP* and that of the merged list of genes selected in (b) and (c) in the TCGA colon, Marisa and Medico studies. (e) Western blot analysis of PrP^C expression in cell extracts from *PRNP*-silenced vs. control MDST8 cells. Protein levels were normalized to α-tubulin (α-tub) (left panel). qRT-PCR analysis of the expression of the selected genes in *PRNP*-silenced vs. control MDST8 cells, normalized relative to *RPL13A* expression (right panel). (f) Western blot analysis of the expression of PrP^C in cell extracts from LoVo cells transfected with pcDNA3-prnp or empty vector for 3 days (left panel). qRT-PCR analysis of the expression of the selected genes in PrP^C-overexpressing vs. control LoVo cells 3 days (Prnp d3) 4 days (Prnp d4) or 5 days (Prnp d5) post-transfection, (right panel). Results are expressed as means of n = 2 independent triplicates of cell preparations ± s.e.m. * $p < .05$, ** $p < .01$, *** $p < .001$ vs. control (Student's *t*-test).

3.5. PrP^C is elevated in metastatic CRC patients plasma and is associated with worse disease control

Having established an association between PrP^C and the poor-prognosis mesenchymal subtype of CRC, we proceeded to evaluate PrP^C as a non-invasive biomarker for CRC, since PrP^C exists as a soluble protein [10]. We selected patients with metastatic CRC from the PRODIGE9 trial [15] whose plasma was available at time of enrolment (Table S2). Although the $n = 325$ out of 488 patients with blood samples were slightly under-represented for WHO performance status ≥2 and high Köhne criteria, they were representative of the cohort in

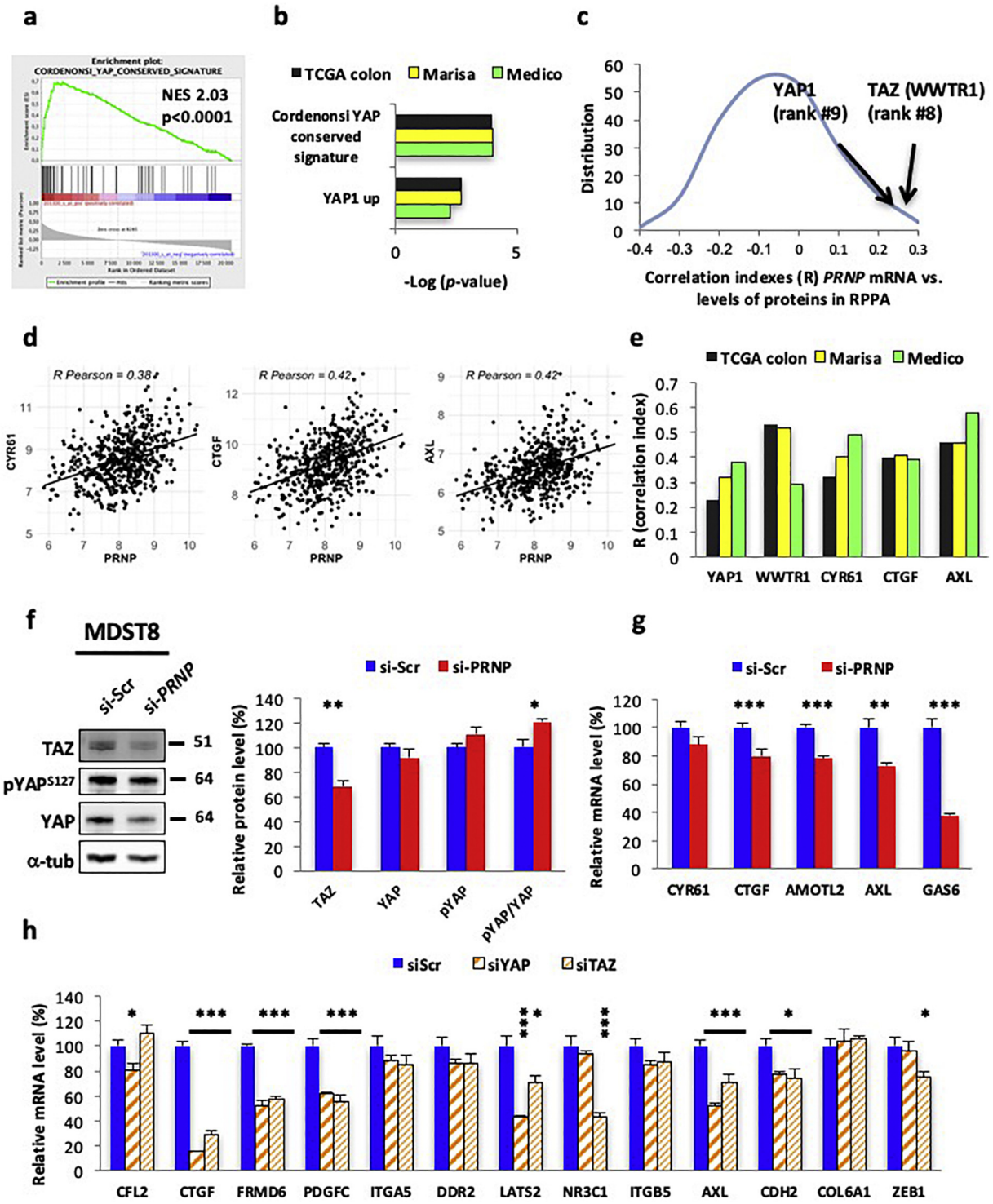

Fig. 3. PrP^C controls C4/CMS4 genes via YAP/TAZ. (a) GSEA analysis showing enrichment of the Cordenonsi YAP conserved signature in the genes most correlated with *PRNP* expression in the Marisa study. (b) Significance expressed as –Log (*p*-values) of the enrichment for the regulation of the Cordenonsi YAP conserved signature and the YAP1 up pathway in the genes most correlated to *PRNP* gene expression in the TCGA colon, Marisa and Medico studies. (c) Analysis of the distribution of the correlation indexes between protein levels and mRNA expression of *PRNP* expression in the TCGA colon study shows enrichment of YAP and TAZ. Pearson's correlation coefficient $R = 0.25$ for YAP and TAZ, $p < .00001$. (d) Analysis of gene expression of a panel of YAP/TAZ targets (*CYR61*, *CTGF* and *AXL*) in the Marisa study demonstrates significant correlations with mRNA expression of *PRNP*. (e) Correlations indexes (R, Pearson) between mRNA expression of *PRNP* and *YAP1*, *WWTR1*, *CYR61*, *CTGF* and *AXL* in the TCGA colon, Marisa and Medico studies. (f) Western blot analysis of the expression of TAZ, phospho-S127-YAP and total YAP in *PRNP*-silenced vs. control MDST8 cells. (g) qRT-PCR analysis of the expression of *CYR61*, *CTGF*, *AMOTL2*, *AXL* and *GAS6* in *PRNP*-silenced vs. control MDST8 cells. (h) qRT-PCR analysis of the expression of C4/CMS4 genes in MDST8 cells transfected with siRNA against YAP or TAZ vs. control MDST8 cells. Results are expressed as means of n = 2 independent triplicates of cell preparations ± s.e.m. * $p < .05$, ** $p < .01$, *** $p < .001$ vs. control (Student's *t*-test).

terms of age, gender, and primary tumour location (Table S4). Patients with metastatic CRC (mCRC) had significantly higher levels of plasma PrP^C than age-matched controls (12.48 ± 9.58 vs. 6.41 ± 1.63 ng/mL, $p < .0005$), with values ranging from 4.40 to 90.40 ng/mL (Fig. 5a). We went on to analyse the association of PrP^C levels with clinical parameters (Table 1). Patients were dichotomized using the first tertile value of PrP^C as threshold in plasmas (8.7 ng/mL). No correlation was found between PrP^C levels and gender, age, WHO performance status, Köhne

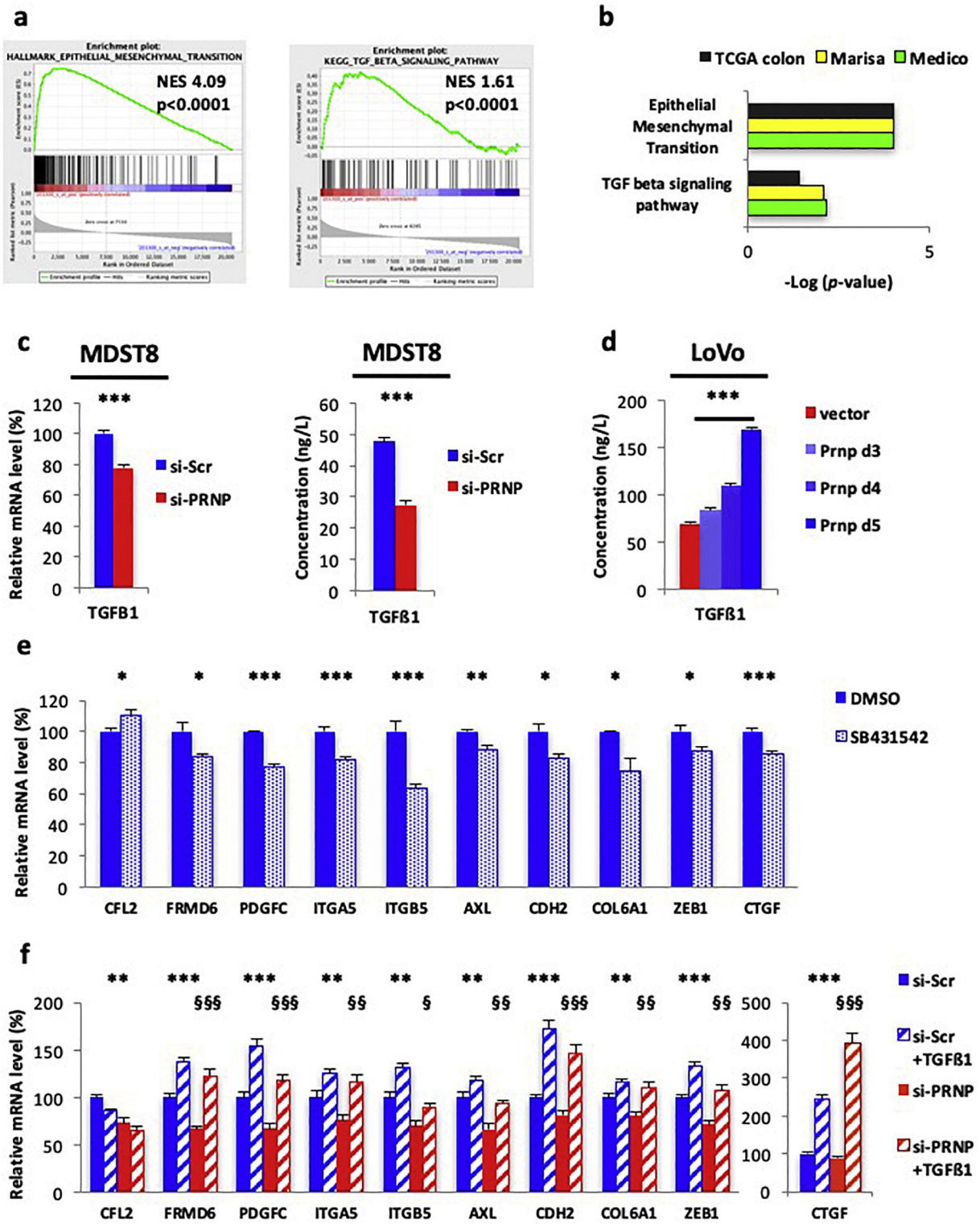

Fig. 4. TGFß signalling participates to the PrP^C – dependent action in C4/CMS4 CRC cells. (a) GSEA analysis showing enrichment of the EMT signature and TGFß pathway in the genes most correlated with *PRNP* expression in the Marisa study. (b) Significance expressed as –Log (*p*-values) of the enrichment for the regulation of the EMT signature and the TGFß signalling pathway in the genes most correlated to *PRNP* gene expression in the TCGA colon, Marisa and the Medico studies. (c) *TGFB1* mRNAs (left) and soluble TGFß1 (right) were measured in *PRNP*-silenced vs. control MDST8 cells. (d) TGFß1 secreted by PrP^C-overexpressing vs. control LoVo cells was measured 3, 4 and 5 days post-transfection. (e) qRT-PCR analysis of the expression of C4/CMS4 genes in SB431542-treated vs. control MDST8. (f) qRT-PCR analysis of the expression of C4/CMS4 genes in MDST8 exposed to siRNA against *PRNP* and recombinant TGFß1. Results are expressed as means of n = 2 independent triplicates of cell preparations ± s.e.m. * $p < .05$, ** $p < .01$, *** $p < .001$ vs. control; § $p < .05$, §§ $p < .01$, §§§ $p < .001$ vs. untreated *PRNP*-silenced MDST8 cells (Student's *t*-test).

criteria, number of metastatic sites or primary tumour location (Table 1). However, in multivariate analysis, high PrP^C levels associated with poor disease control, which is the primary endpoint of the PRODIGE9 study [16] (HR = 1.53, 95%CI = 1.07 to 2.18, $p < .05$, Fig. 5b and c). A tendency towards poor overall survival and progression-free survival was also observed, although not reaching

significance (Fig. 5b and Fig. S5a and b). Since high Köhne criteria is associated with poor prognosis ([26] and (Fig. S6a)), we restricted our analyses on patients with low and medium Köhne criteria, who have similar disease control (Fig. S6a). We confirmed the significant worse outcome of high PrP^C levels in terms of disease control (HR = 1.64, 95%CI = 1.10 to 2.46, $p < .05$, Fig. 5d) and the trend towards poorer OS and PFS (Fig. S6b and c). Overall, these data suggest that high PrP^C levels predict disease control in metastatic CRC.

4. Discussion

The present work introduces PrP^C as a candidate driver of the C4/CMS4 phenotype in CRC and a potential prognostic biomarker for disease control in mCRC. While considerable attention has been paid to PrP for its involvement in neurodegeneration [9], still little is known on its contribution to tumour progression. PrP^C overexpression has been reported in several types of cancer, including breast, colon, gastric and pancreatic cancer [27]. A consensus view is that increased levels of PrP^C endow cells with proliferative [28–30], migratory and invasive capacities [31–33], as well as with increased resistance to anti-cancer agents [34,35]. Very recently, secreted PrP^C was shown to bind doxorubicin and to correlate with anthracycline resistance in breast cancer [36]. Few studies have also uncovered a link between PrP^C and CSC (reviewed in [8]). Despite this overall advance, a comprehensive view of the molecular pathways through which PrP^C takes part to these cellular processes is still lacking.

One possible obstacle in the quest for a better understanding of the contribution of PrP^C to cancer progression may be tumour heterogeneity. Indeed, in the past few years, it has become clear that many cancers, including CRC, can exhibit diverse molecular landscapes [37]. Mining the distribution of *PRNP* expression across the diverse subtypes allowed us to uncover a specific up-regulation of the expression of this gene in the C4 [3] or CMS4 [7] subtypes, both characterized by poor prognoses. In line with this, we found that high *PRNP* mRNA levels are associated with significantly reduced overall survival and relapse-free survival.

The other specific features of the C4/CMS4 related subtypes include CSC and EMT hallmarks, enrichment for the TGFß pathway, and increased resistance to 5-FU treatment [3,7,19]. Importantly, our in vitro data obtained with the C4/CMS4 MDST8 cell line reveal that PrP^C silencing attenuates these overall characteristics, arguing that PrP^C may represents one of the protagonists that drive the C4/CMS4 phenotype. Conversely, PrP^C overexpression in the C2/CMS1 LoVo cell line promotes an increase in soluble TGFß1 and exacerbates the expression of a set of C4/CMS4 genes. From a mechanistic point of view, we identify a PrP^C -YAP/TAZ axis, which controls the expression of C4/CMS4 genes. Several studies have exemplified an involvement of YAP/TAZ in colon cancer

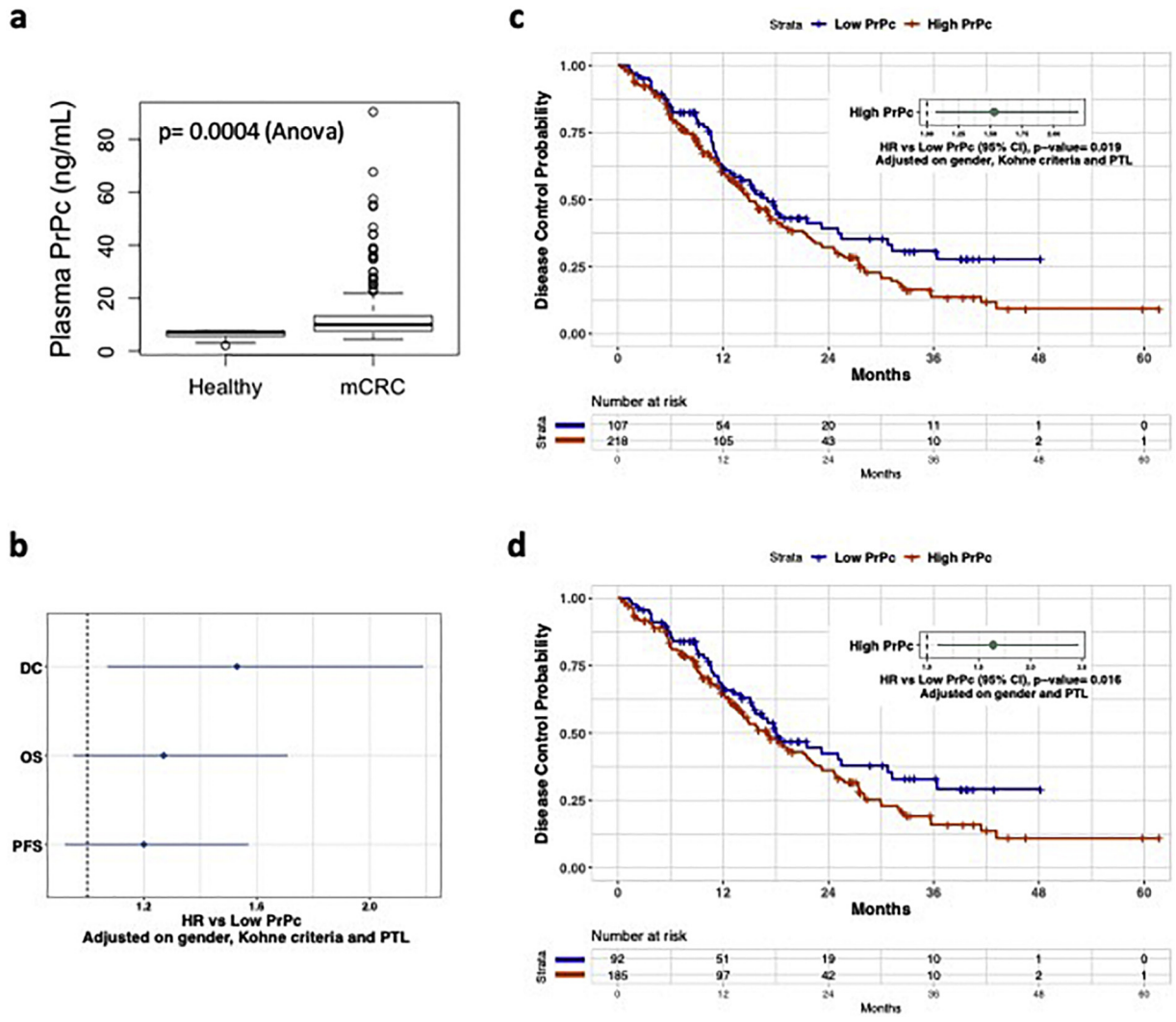

Fig. 5. PrP^C is elevated in the plasma of metastatic CRC patients and is associated with poor disease control. (a) Plasma levels of PrP^C measured in n = 32 healthy subjects and n = 325 patients with mCRC. (b) Summary of multivariate analyses of PrP^C high vs. low samples for disease control (DC), progression-free survival (PFS), overall survival (OS) for all patients tested ($n = 325$). Dichotomization of patients by PrP^C was at 8.7 ng/mL. Analyses were adjusted on gender, Köhne criteria and primary tumour location. (c-d) Kaplan-Meier disease control probability according to PrP^C plasma levels in all patients tested (n = 325) (c) or in patients with low or intermediate Köhne criteria (n = 277) (d).

Table 1
Patient characteristics from PRODIGE 9 study according to plasma PrP^C levels.

		Low PrP^C	High PrP^C	Total	*p*-Value
		$n = 107$	$n = 218$	$n = 325$	
Gender	Male	68	144	212	$p = .748$[a]
	Female	39	74	113	
Age	Mean	65.38	64.23	65.28	$p = .688$[b]
	Range	42.98–83.96	26.87–88.76	26.87–88.76	
PT resected	Yes	69	121	190	$p = .127$[a]
	No	37	97	134	
WHO performance status	0	58	101	159	$p = .148$[a]
	1	41	107	148	
	2	8	10	18	
Köhne criteria	Low	41	85	126	$p = .942$[a]
	Intermediate	51	100	151	
	High	15	33	48	
Metastatic sites	1	45	88	133	$p = .864$[a]
	>1	62	130	192	
PTL	Proximal	22	56	78	$p = .452$[a]
	Distal	61	119	180	
	NA	24	43	67	
Treatment during chemotherapy-free interval	Bevacizumab maintenance	56	109	165	$p = .781$[a]
	Observation	51	109	160	

PT: primary tumour, PTL: primary tumour location.
[a] Chi-square test.
[b] Wilcoxon test.

and depicted correlations between elevated YAP or TAZ levels and poor prognoses in CRC patients (reviewed in [38,39]). However, despite the significant enrichment of YAP and TAZ proteins in the CMS4 subgroup [7], this is, to our knowledge, the first demonstration that YAP/TAZ can take part to the specification of the C4/CMS4 subtype. As a whole, by uncovering a link between PrP^C, YAP/TAZ and the TGFß pathway, our work provides a molecular scenario through which PrP^C would sustain the emergence and/or maintenance of the C4/CMS4 phenotype in CRC.

Another important contribution of our study is the demonstration that plasma levels of PrP^C can discriminate patients with poor disease control in metastatic CRC. These findings are consistent with the view that elevated PrP^C, as found in C4/CMS4 tumours, would favour metastatic dissemination and/or progression. Although one limitation of our results is the exploratory, retrospective nature of the analysis, they are strengthened by the large size of the cohort, long-term follow-up data and the multi-centric collection of samples. We suggest that plasma PrP^C measurement may notably help the prognostication of disease control in patients with low or intermediate Köhne criteria, i.e. those with best outcome among metastatic CRC patients.

As a conclusion, our findings warrant further investigating whether PrP^C could constitute a relevant target for the treatment of mesenchymal-like CRC as well as a potential marker for patient stratification in CRC.

Supplementary data to this article can be found online at https://doi.org/10.1016/j.ebiom.2019.07.036.

Acknowledgements

We thank M. Bühler for expert methodological assistance and S. Lehmann for the pcDNA3-Prnp plasmid. R.B. was supported by a fellowship form Institut National du Cancer.

Funding sources

Grant support was provided by the following: Cancéropôle Ile de France (grant number 2016-1-EMERG-36-UP 5-1), Association pour la Recherche sur le Cancer (grant number PJA 20171206220), SATT Ile de France Innov (grant number 415) as well as INSERM. The funders had no role in study design, data collection, data analysis, interpretation or writing of the report.

Declaration of Competing Interests

The authors declare no competing interests in the present study.

Author contributions

D.L-C., A.G., R.B., C.P., S.M-L., L.M., and F.D.: collection and assembly of data, data analysis and interpretation and final approval of the manuscript; T.A., V.P., C.M., K.L.M., J.T., F.G. and J.B.: data or human sample collection and final approval of the manuscript; C.C.: material support; J-F. E, V.B., H.B. and A.D-R.: data analysis and interpretation and final approval of the manuscript; J-M.L: collection and assembly of data, financial support, data analysis and interpretation and final approval of the manuscript; P.L-P.: conception and design, financial support, data analysis and interpretation and final approval of the manuscript. S.M-R.: conception and design, financial support, collection and assembly of data, data analysis and interpretation, manuscript writing.

References

[1] Budinska E, Popovici V, Tejpar S, D'Ario G, Lapique N, Sikora KO, et al. Gene expression patterns unveil a new level of molecular heterogeneity in colorectal cancer. J Pathol 2013;231:63–76. https://doi.org/10.1002/path.4212.
[2] De Sousa E, Melo F, Wang X, Jansen M, Fessler E, Trinh A, et al. Poor-prognosis colon cancer is defined by a molecularly distinct subtype and develops from serrated precursor lesions. Nat Med 2013;19:614–8. https://doi.org/10.1038/nm.3174.
[3] Marisa L, de Reynies A, Duval A, Selves J, Gaub MP, Vescovo L, et al. Gene expression classification of colon cancer into molecular subtypes: characterization, validation, and prognostic value. PLoS Med 2013;10:e1001453. https://doi.org/10.1371/journal.pmed.1001453.
[4] Roepman P, Schlicker A, Tabernero J, Majewski I, Tian S, Moreno V, et al. Colorectal cancer intrinsic subtypes predict chemotherapy benefit, deficient mismatch repair and epithelial-to-mesenchymal transition. Int J Cancer 2014;134:552–62. https://doi.org/10.1002/ijc.28387.
[5] Sadanandam A, Lyssiotis CA, Homicsko K, Collisson EA, Gibb WJ, Wullschleger S, et al. A colorectal cancer classification system that associates cellular phenotype and responses to therapy. Nat Med 2013;19:619–25. https://doi.org/10.1038/nm.3175.
[6] Schlicker A, Beran G, Chresta CM, McWalter G, Pritchard A, Weston S, et al. Subtypes of primary colorectal tumors correlate with response to targeted treatment in colorectal cell lines. BMC Med Genomics 2012;5:66. https://doi.org/10.1186/1755-8794-5-66.
[7] Guinney J, Dienstmann R, Wang X, de Reyniès A, Schlicker A, Soneson C, et al. The consensus molecular subtypes of colorectal cancer. Nat Med 2015;21:1350–6. https://doi.org/10.1038/nm.3967.
[8] Martin-Lannerée S, Hirsch TZ, Hernandez-Rapp J, Halliez S, Vilotte JL, Launay JM, et al. PrPC from stem cells to cancer. Front Cell Dev Biol 2014;2:55.

[9] Aguzzi A, Calella AM. Prions: protein aggregation and infectious diseases. Physiol Rev 2009;89:1105–52.
[10] Hirsch TZ, Martin-Lannerée S, Mouillet-Richard S. Functions of the prion protein. Prog Mol Biol Transl Sci 2017;150:1–34. https://doi.org/10.1016/bs.pmbts.2017.06.001.
[11] Malaga-Trillo E, Solis GP, Schrock Y, Geiss C, Luncz L, Thomanetz V, et al. Regulation of embryonic cell adhesion by the prion protein. PLoS Biol 2009;7:e55.
[12] Subramanian A, Tamayo P, Mootha VK, Mukherjee S, Ebert BL, Gillette MA, et al. Gene set enrichment analysis: a knowledge-based approach for interpreting genome-wide expression profiles. Proc Natl Acad Sci U S A 2005;102:15545–50. https://doi.org/10.1073/pnas.0506580102.
[13] Cancer Genome Atlas Network. Comprehensive molecular characterization of human colon and rectal cancer. Nature 2012;487:330–7. https://doi.org/10.1038/nature11252.
[14] Medico E, Russo M, Picco G, Cancelliere C, Valtorta E, Corti G, et al. The molecular landscape of colorectal cancer cell lines unveils clinically actionable kinase targets. Nat Commun 2015;6:7002. https://doi.org/10.1038/ncomms8002.
[15] Aparicio T, Linot B, Le Malicot K, Bouché O, Boige V, François E, et al. FOLFIRI +bevacizumab induction chemotherapy followed by bevacizumab or observation in metastatic colorectal cancer, a phase III trial (PRODIGE 9–FFCD 0802). Dig Liver Dis Off J Ital Soc Gastroenterol Ital Assoc Study Liver 2015;47:271–2. https://doi.org/10.1016/j.dld.2015.01.146.
[16] Aparicio T, Ghiringhelli F, Boige V, Le Malicot K, Taieb J, Bouché O, et al. Bevacizumab maintenance versus no maintenance during chemotherapy-free intervals in metastatic colorectal cancer: a randomized phase III trial (PRODIGE 9). J Clin Oncol Off J Am Soc Clin Oncol 2018;36:674–81. https://doi.org/10.1200/JCO.2017.75.2931.
[17] MacGregor I, Hope J, Barnard G, Kirby L, Drummond O, Pepper D, et al. Application of a time-resolved fluoroimmunoassay for the analysis of normal prion protein in human blood and its components. Vox Sang 1999;77:88–96. https://doi.org/10.1159/000031082.
[18] Calon A, Lonardo E, Berenguer-Llergo A, Espinet E, Hernando-Momblona X, Iglesias M, et al. Stromal gene expression defines poor-prognosis subtypes in colorectal cancer. Nat Genet 2015;47:320–9. https://doi.org/10.1038/ng.3225.
[19] Sveen A, Bruun J, Eide PW, Eilertsen IA, Ramirez L, Murumägi A, et al. Colorectal cancer consensus molecular subtypes translated to preclinical models uncover potentially targetable cancer cell dependencies. Clin Cancer Res Off J Am Assoc Cancer Res 2018;24:794–806. https://doi.org/10.1158/1078-0432.CCR-17-1234.
[20] Roumeliotis TI, Williams SP, Gonçalves E, Alsinet C, Del Castillo Velasco-Herrera M, Aben N, et al. Genomic determinants of protein abundance variation in colorectal cancer cells. Cell Rep 2017;20:2201–14. https://doi.org/10.1016/j.celrep.2017.08.010.
[21] Bracht K, Nicholls AM, Liu Y, Bodmer WF. 5-Fluorouracil response in a large panel of colorectal cancer cell lines is associated with mismatch repair deficiency. Br J Cancer 2010;103:340–6. https://doi.org/10.1038/sj.bjc.6605780.
[22] Varelas X. The Hippo pathway effectors TAZ and YAP in development, homeostasis and disease. Dev Camb Engl 2014;141:1614–26. https://doi.org/10.1242/dev.102376.
[23] Lian I, Kim J, Okazawa H, Zhao J, Zhao B, Yu J, et al. The role of YAP transcription co-activator in regulating stem cell self-renewal and differentiation. Genes Dev 2010;24:1106–18. https://doi.org/10.1101/gad.1903310.
[24] Zanconato F, Forcato M, Battilana G, Azzolin L, Quaranta E, Bodega B, et al. Genome-wide association between YAP/TAZ/TEAD and AP-1 at enhancers drives oncogenic growth. Nat Cell Biol 2015;17:1218–27. https://doi.org/10.1038/ncb3216.
[25] Gregorieff A, Liu Y, Inanlou MR, Khomchuk Y, Wrana JL. Yap-dependent reprogramming of Lgr5(+) stem cells drives intestinal regeneration and cancer. Nature 2015;526:715–8. https://doi.org/10.1038/nature15382.
[26] Desot E, de Mestier L, Volet J, Delmas C, Garcia B, Geoffroy P, et al. Prognostic factors in patients with non resectable metastatic colorectal cancer in the era of targeted biotherapies: relevance of Köhne's risk classification. Dig Liver Dis Off J Ital Soc Gastroenterol Ital Assoc Study Liver 2013;45:330–5. https://doi.org/10.1016/j.dld.2012.10.016.
[27] Mehrpour M, Codogno P. Prion protein: from physiology to cancer biology. Cancer Lett 2010;290:1–23. https://doi.org/10.1016/j.canlet.2009.07.009.
[28] Cheng Y, Tao L, Xu J, Li Q, Yu J, Jin Y, et al. CD44/cellular prion protein interact in multidrug resistant breast cancer cells and correlate with responses to neoadjuvant chemotherapy in breast cancer patients. Mol Carcinog 2013;53:686–97. https://doi.org/10.1002/mc.22021.
[29] Lopes MH, Santos TG, Rodrigues BR, Queiroz-Hazarbassanov N, Cunha IW, Wasilewska-Sampaio AP, et al. Disruption of prion protein-HOP engagement impairs glioblastoma growth and cognitive decline and improves overall survival. Oncogene 2014;34:3305–14. https://doi.org/10.1038/onc.2014.261.
[30] Provenzano L, Ryan Y, Hilton DA, Lyons-Rimmer J, Dave F, Maze EA, et al. Cellular prion protein (PrPC) in the development of Merlin-deficient tumours. Oncogene 2017;36:6132–42. https://doi.org/10.1038/onc.2017.200.
[31] Du L, Rao G, Wang H, Li B, Tian W, Cui J, et al. CD44-positive cancer stem cells expressing cellular prion protein contribute to metastatic capacity in colorectal cancer. Cancer Res 2013;73:2682–94. https://doi.org/10.1158/0008-5472.CAN-12-3759.
[32] Iglesia RP, Prado MB, Cruz L, Martins VR, Santos TG, Lopes MH. Engagement of cellular prion protein with the co-chaperone Hsp70/90 organizing protein regulates the proliferation of glioblastoma stem-like cells. Stem Cell Res Ther 2017;8:76. https://doi.org/10.1186/s13287-017-0518-1.
[33] de Lacerda TCS, Costa-Silva B, Giudice FS, Dias MVS, de Oliveira GP, Teixeira BL, et al. Prion protein binding to HOP modulates the migration and invasion of colorectal cancer cells. Clin Exp Metastasis 2016;33:441–51. https://doi.org/10.1007/s10585-016-9788-8.
[34] Chieng CK-L, Say Y-H. Cellular prion protein contributes to LS 174T colon cancer cell carcinogenesis by increasing invasiveness and resistance against doxorubicin-induced apoptosis. Tumour Biol J Int Soc Oncodeve Biol Med 2015;36:8107–20. https://doi.org/10.1007/s13277-015-3530-z.
[35] Lee JH, Yun CW, Lee SH. Cellular prion protein enhances drug resistance of colorectal cancer cells via regulation of a survival signal pathway. Biomol Ther 2018;26:313–21. https://doi.org/10.4062/biomolther.2017.033.
[36] Wiegmans AP, Saunus JM, Ham S, Lobb R, Kutasovic JR, Dalley AJ, et al. Secreted cellular prion protein binds doxorubicin and correlates with anthracycline resistance in breast cancer. JCI Insight 2019;5. https://doi.org/10.1172/jci.insight.124092.
[37] Dienstmann R, Vermeulen L, Guinney J, Kopetz S, Tejpar S, Tabernero J. Consensus molecular subtypes and the evolution of precision medicine in colorectal cancer. Nat Rev Cancer 2017;17:268. https://doi.org/10.1038/nrc.2017.24.
[38] Hong AW, Meng Z, Guan K-L. The Hippo pathway in intestinal regeneration and disease. Nat Rev Gastroenterol Hepatol 2016;13:324–37. https://doi.org/10.1038/nrgastro.2016.59.
[39] Zanconato F, Cordenonsi M, Piccolo S. YAP/TAZ at the roots of cancer. Cancer Cell 2016;29:783–803. https://doi.org/10.1016/j.ccell.2016.05.005.